

# Miniaturized Frequency Selective Radome Operating in the X-Band with Wideband Absorption

Hamza Ahmad<sup>1</sup>, MuhibUr Rahman<sup>2\*</sup>, Shahid Bashir<sup>3</sup>, Wajid Zaman<sup>4</sup>,  
and Fauziahanim Che Seman<sup>5</sup>

<sup>1</sup> Gandhara Institute of Science and Technology, Peshawar, Pakistan

<sup>2\*</sup>Department of Electrical Engineering, Polytechnique Montreal, Montreal, QC H3T 1J4, Canada

<sup>3</sup>University of Engineering and Technology, Peshawar, Pakistan

<sup>4</sup>National University of Sciences & Technology (NUST), Islamabad, Pakistan

<sup>5</sup>Research Center of Applied Electromagnetics, Universiti Tun Hussein Onn Malaysia, Batu Pahat, Malaysia

**Abstract** — In this work, a miniaturized frequency selective radome with wideband absorption is presented. The proposed design consists of a bandpass FSS and a resistive FSS. Both FSS's are combined together through a foam spacer. A slotted miniaturized form of the conventional Jerusalem cross structure is employed as the bandpass FSS. A meandered form of the basic square loop with lumped resistors incorporated in each side of the loop is used as the resistive FSS. The bandpass FSS ensures the transmission in the X-band, which is the operating band of the radome. The resistive FSS absorbs the out-of-band signals and thus reduces RCS at higher frequencies. The proposed design operates in the frequency range of 8.88-10.85 GHz and absorbs between 18.8-28.35 GHz. The insertion loss at the center frequency of the operating band is 0.82 dB. The thickness of the entire structure is  $0.07 \lambda_0$  with respect to center frequency (10 GHz) of the operating band. The overall size of a unit cell of the miniaturized design is  $0.2 \lambda_0$  that ensure angular stability for different polarizations and incident angles.

**Index Terms** — Bandpass FSS, Frequency Selective Surface (FSS), radome, resistive FSS, wideband absorption.

## I. INTRODUCTION

A radome is usually made up of weatherproof material and used as a shield for an antenna to protect it from the physical environment. It is necessary for a radome to have a negligible effect on the operating frequency of encircled antenna so that electrical performance of antenna may not be disturbed. Radomes having frequency selective abilities have attracted the designers in recent years. Such radomes have the

tendency to prevent coupling from nearby antenna without disturbing radiation characteristics of the antenna [1,2]. Frequency selective surfaces (FSSs) are employed for this purpose. FSSs possesses spatial filtering properties and usually have a periodic structure. A radome is normally considered as a bandpass FSS which permits the passage of operating signal with negligible insertion loss and blocks the unwanted signal [3,4].

The radar cross section (RCS) of an object is its equivalent area which if scattered isotropically would result in the same scattered power density. With the development of the radar detection and stealth technology, how to reduce RCS has been of great military and practical significance. Over the years, there has been a growing attraction in the design of stealthy radome for many applications. Stealth technology requires the reduction of radar cross section of the antenna without affecting its radiation capabilities [5]. An antenna contributes in the in-band RCS and out-of-band RCS, depending on the radome reflection characteristics and its geometry. The RCS of the antenna can be reduced when frequency selective radome, designed with proper geometry, reflects the incident out of band signal in specular directions. Monostatic RCS of antenna which has not additional scatterers in its proximity can be reduced through this technique [6-7]. However, this technique cannot reduce the bistatic RCS because the reflected signal can be collected by bistatic radars.

An ideal condition for low RCS radome is that the desired signal must have minimum attenuation, whereas the incident unwanted signal should be absorbed. In [8], this concept has been proposed by introducing an absorbing layer in the structure. However, the qualitative

results are not provided. A bandpass filter is achieved by a conductive FSS while the absorption of out of band signal is achieved through bandstop resistive FSS [9]. The bandpass and resistive FSS are providing wideband absorption with different geometries. In [10], a conductive FSS and a resistive FSS with lumped resistors are used to form a composite structure. In [11], two resonators are coupled to miniaturize a bandstop FSS for wideband rejection.

In [12], they have proposed a novel FSS reflector for a dipole array to mitigate RCS within operating frequency range. The proposed FSS possesses good bandstop characteristics and is designed on quasi fractal geometrical approach which is quite complex to implement. Similarly in [13], FSS radome is designed using binary particle swarm optimization (BPSO) algorithm by the combination of pixel overlap technique. The proposed technique is quite attractive, however the manufacturability of this design become limited as the lattice points in FSS element are difficult to avoid from neighboring conductors, which in fact creates the overlapping problem. In [14], a switchable wideband FSS absorber/reflector is designed for C-band applications operating within 4-8 GHz frequency range. The proposed FSS has innovative characteristics by combining switchable performance with wideband absorption. In [15], a wideband rasorber is designed which operates at 3.8-10.3 GHz with and incorporates the switching of transmission and reflection bands using pin diodes. Triple-layer FSS has been used in [16] for a wide transmission band with a resistive sheet for absorption at lower frequencies. Another design with similar operation has been presented in [17] using dipole arrays. An FSS based rasorber with meander line square loop having lumped resistors has been presented in [18] while a dual absorption band has been achieved in [19]. A frequency selective radome for the X-band has been designed by combining a bandpass FSS and an absorbing FSS using the surface resistive technique [20].

In this work, an FSS based radome with frequency selective capabilities is designed. The proposed design consists of a miniaturized bandpass FSS that permits the operating signal to pass through the structure unattenuated while reflecting any out-of-band signal. The proposed design also consists of a miniaturized resistive FSS with lumped resistors to absorb the unwanted signal. This aids in minimizing the RCS of antenna that would be enclosed in the proposed radome. The operating band is chosen to be X-band which is used in radar applications and space communication. The absorption band covers frequencies above the X-band to make the antenna, enclosed in the radome, invisible to a potential target. This design is better than [20] due to several reasons. Firstly, a parametric analysis of the

design parameters is presented in this work. Secondly, the equivalent circuit for the proposed design is given with the values of circuit elements. Finally, the angular stability for this design is better than [20] and thus can give desired response even for oblique incident signals.

## II. PROPOSED DESIGN

The proposed unit cell design is demonstrated in Fig. 1. A resistive FSS is placed on the front side while a bandpass FSS is placed on the back side of the structure. The bandpass and the resistive FSS are designed separately on two identical substrates. The material employed as substrate is RT/Duroid 5880 ( $\epsilon_r = 2.2$ ) with a thickness of 0.127mm. Both the FSSs are separated by a foam spacer. The overall thickness and periodicity of the proposed design have been carefully optimized.

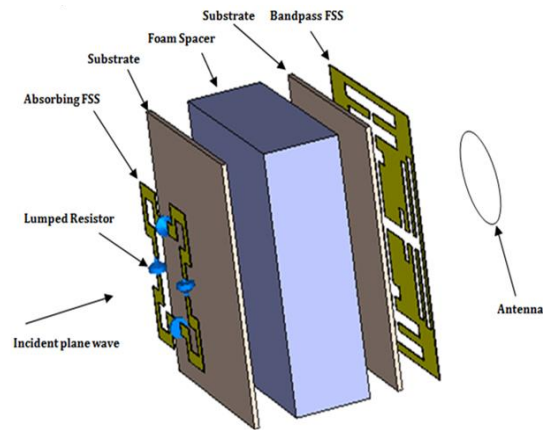


Fig. 1. Proposed unit cell structure of the FSS based radome.

The presented design is represented by the equivalent circuit illustrated in Fig. 2. The bandpass FSS is represented by a parallel LC circuit while the resistive FSS is represented by a series RLC circuit. The thickness of the foam spacer is represented by a transmission line of length  $d$ . The resistance,  $R$  comes from the resistors inserted in the four sides of the resistive FSS. Absorption of signals requires that there is no reflected signal from the proposed structure. Therefore, the input impedance of the proposed structure should be equal to the free space impedance,  $Z_0$ . The controlling parameters to achieve this goal are the resistance  $R$  and the thickness  $d$  of the foam spacer. Initially, the bandpass FSS and resistive FSS are designed. The resistance and thickness of the foam spacer are then optimized so that the imaginary part of the input impedance of the proposed design becomes zero while the real part becomes close to  $377 \Omega$  to ensure perfect absorption in the required band.

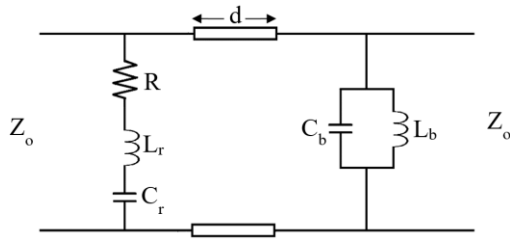


Fig. 2. Equivalent circuit of the proposed design.

### III. BANDPASS FSS

We need to design the bandpass FSS in such a way that it has a passband in the operating frequency of the proposed structure and also a wide reflection bandwidth. The unit cell structure for the bandpass FSS is illustrated in Fig. 3 which is a modified form of the conventional slotted Jerusalem cross structure [2]. It is designed to give a passband in the X-band and reflects higher frequencies. The Jerusalem Cross resonates when the end to end length is approximately  $\lambda/2$ . Starting from this, the element is modified and miniaturized to resonate at the desired frequency but with a small size. The greater inter-element spacing and smaller periodicity of this miniaturized structure prevent grating lobes and make the structure narrowband.

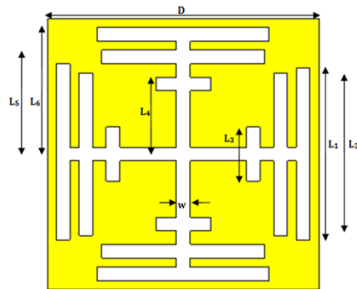


Fig. 3. Unit cell of the bandpass FSS.  $D = 6$  mm,  $L_1 = 3.8$  mm,  $L_2 = 3.6$  mm,  $L_3 = 1.2$  mm,  $L_4 = 1.7$  mm.

### IV. RESISTIVE FSS

In order to achieve a large bandwidth in the absorption band, the preferred element for the resistive FSS is the basic square loop [2]. While designing the resistive FSS, it must be ensured that the insertion loss in the operating band of the antenna does not increase. The basic loop resonates when the circumference of the loop is approximately one wavelength. For absorption at lower frequencies, the size of the square loop is to be kept large, but this causes an increase in the insertion loss in the operating band. This complication can be catered by miniaturizing the basic square loop structure via meandering [21] as shown in Fig. 4. The absorption capability in this bandstop FSS is achieved by incorporating lumped resistors into the four sides of the loop.

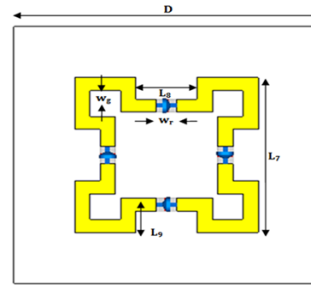


Fig. 4. Unit cell of the resistive FSS.  $D = 6$  mm,  $L_7 = 3.6$  mm,  $L_8 = 1.2$  mm,  $L_9 = 0.7$  mm,  $w_r = 0.4$  mm,  $w_g = 0.3$  mm.

### V. ANALYSIS AND RESULTS

The proposed design is simulated in CST microwave studio using unit cell boundary conditions. The structure needs to be analyzed both in transmitting and receiving modes for the performance of a practical radome. For an incoming wave on the front side of the design, the transmission and reflection coefficients for both modes are shown in Fig. 5. The operating band is from 8.88-10.85 GHz. The center frequency is 10 GHz where the insertion loss is only 0.82dB. The frequency band between 18.8-28.35 GHz is the absorption band of the radome. The absorption band can be shifted to a lower frequency at the cost of increased insertion loss in the operating band. The transmission coefficient in the transmitting and receiving modes are exactly the same which is the case for every passive device. However, the reflection coefficients of both the modes are different from each other. The reason for this phenomenon is that the out-of-band signal is absorbed in receiving mode while it is totally reflected in transmitting mode.

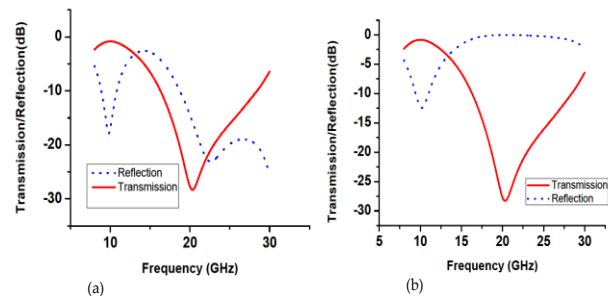


Fig. 5. Transmission and reflection coefficient of radome: (a) receiving mode and (b) transmitting mode.

Figure 6 exhibits the absorption percentages for transmitting and receiving modes. It is evident that absorption is greater than 80% between 18.8-28.35 GHz in the receiving mode. Absorption is negligible in the same band for transmitting mode. These results confirm the absorption performance of the proposed radome. A practical radome requires that the passband transmission is stable with the incidence angle. The small periodicity

of the structure guarantees passband stability, but the absorption properties are degraded with the incidence angle.

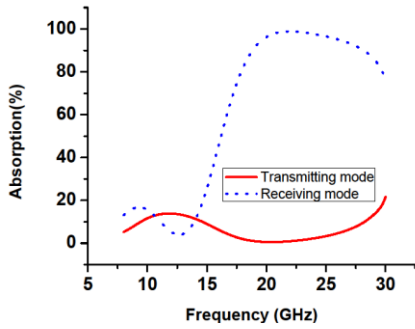


Fig. 6. Absorption percentage of radome.

Figure 7 manifests the transmission and reflection coefficients in receiving mode of the radome for various incident angles of TE and TM polarizations. The reflection and transmission coefficients are stable up to 45°. The stability can be improved for higher incidence angles by increasing the lumped resistance. This, unfortunately, increases the insertion loss in the passband. The operating band is stable for both TE and TM polarizations. The absorbing bandwidth decreases with increase in angle of incidence. For TM polarization, the absorbing bandwidth is reduced much drastically as compared to TE polarization as the incidence angle goes higher.

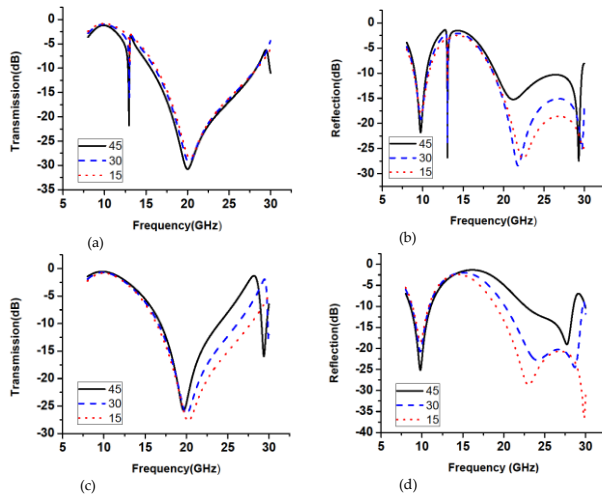


Fig. 7. Transmission and reflection coefficients for oblique incidence angles: (a) transmission for TE polarization, (b) reflection for TE polarization, (c) transmission for TM polarization, and (d) reflection for TM polarization.

The value of the lumped resistance for the proposed design is optimized to 120 Ω through parametric sweeps.

Figure 8 shows the effect of different values of ‘R’ on reflection and transmission coefficients in receiving mode of the radome. We need to choose that value of resistance which gives us smaller insertion loss in the working band and larger absorption in the absorption band. For resistance values less than 120 Ω, the insertion loss is smaller but the reflection coefficient is higher in the absorption band as compared to values greater than 120Ω. Therefore, the value of 120 Ω is a good compromise keeping in view all the aspects.

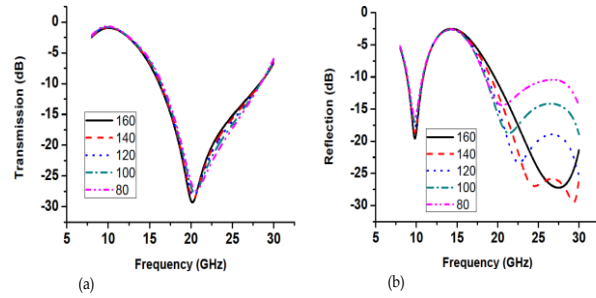


Fig. 8. Effect of different values of lumped resistance, R: (a) transmission and (b) reflection.

The thickness, d, of the foam spacer is critical to the performance of the proposed design. Figure 9 shows the effect of different values of the thickness of the spacer on the transmission and reflection coefficients. For our design, we require that the transmission coefficient in the operating band be closer to 0 dB. At the same time, we need the absorption bandwidth to be as large as possible. Careful observation of Fig. 9 indicates that a thickness of 2mm is the best choice to meet our criteria.

The thickness of the overall design is only 2.3mm and the periodicity of the unit cell is 6mm. The values of the circuit components at the center frequency of the operating band have been found to be  $L_b = 0.26$  nH,  $C_b = 0.98$  pF,  $d = 2$  mm,  $L_r = 1.61$  nH,  $C_r = 0.16$  pF,  $R = 120$  Ω. Table 1 gives a performance comparison of our work with some of the designs reported previously in literature

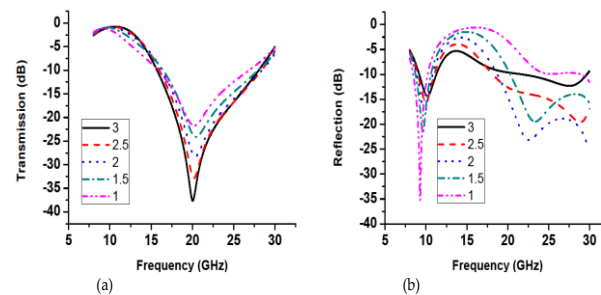


Fig. 9. Effect of different values of spacer thickness “d”: (a) transmission and (b) reflection.

Table 1: Performance comparison of several FSS

Ref.	Transmission Band (GHz)	Absorption Band (GHz)	Polarization	FSS Type
[9]	3 - 5	10 - 18	Double	Interdigital Jerusalem Cross elements
[10]	0.85 - 0.95	3 - 9	Double	Incurved square loops loaded with lumped resistors
[15]	2.80 - 2.90	3.8 - 10.3	Double	Square loop with lumped resistors and PIN diodes
[16]	8.3 - 11.07	2.4 - 7.1	Double	Circular spiral resonators with lumped resistors
[17]	5.2 - 5.8 GHz	2.8 - 5.0	Double	Crossed dipole with lumped resistor
[22]	23.5 GHz to 24.6 GHz	0 to 30 GHz excluding 23.5 to 24.6 GHz	Double	Slotted rings
[23]	4.09 - 4.90	1.98 - 4.70	Double	Square loop with lumped resistors
[24]	4.6 - 5.8	2.3 - 7.2	Single	Four leg loaded cross element
[25]	4.68 - 5.36	2.66 - 4.5 5.66 - 8.56	Single	Tripole loop and tripole slots
Our work	10 GHz	18.8 - 28.3 GHz	Double	Meandered square loop with lumped resistors

## VI. EXPERIMENTAL SETUP

The proposed radome was measured in an anechoic chamber by using Keysight N5234A with the time-domain gating. The aperture of two horn antennas for testing is 65mm×65mm. The space between transmitting antenna (TX) or receiving antenna (RX) and the radome was 0.8 m. Due to the measurement setup limitation, the far-field condition was hard to meet for the entire frequency range. Our prototype was positioned on the far field of the TX antennas so that the transmission can be considered similar to the simulation. As a result, some discrepancy could arise concerning the reflection effects at the higher frequencies. The radome was surrounded with absorbent foam to reduce the effect of the edge diffraction. The corresponding unit cell prototype and measured transmission and reflection coefficient of radome in receiving and transmitting mode is shown in Figs. 10 (a) and (b), respectively.

## VII. CONCLUSION

A frequency selective radome having a miniaturized unit cell with broadband absorption has been presented. The operating band of the proposed design is X-band while the absorption occurs at higher frequencies. An alteration of the basic Jerusalem cross structure is used as a bandpass FSS for transmission. For absorption, the basic square loop is miniaturized and meandered consisting of lumped resistors, is used as a resistive FSS. The operating band is from 8.88-10.85 GHz. The center frequency is 10 GHz where the insertion loss is only 0.82dB. The frequency band between 18.8-28.35 GHz is the absorption band of the radome. At the operating frequency of the proposed design, the thickness is  $0.07 \lambda_0$ . The periodicity of the unit cell of the proposed design

is kept small in order to suppress grating lobes in the absorption band. The angular stability for the proposed design is up to 45° for each TE and TM polarizations.

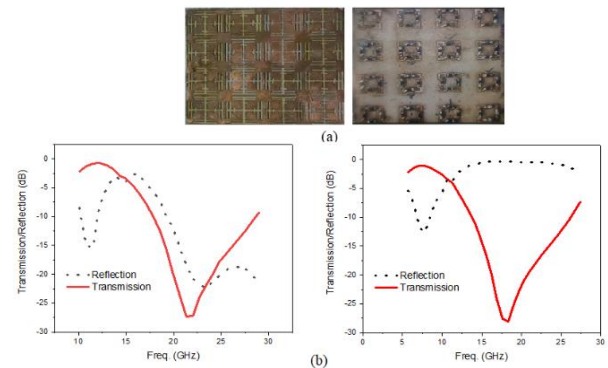


Fig. 10. (a) Unit cell prototype, and (b) measured transmission and reflection coefficient of radome in receiving and transmitting mode.

## REFERENCES

- [1] D. J. Kozakoff, *Analysis of Radome-Enclosed Antennas*. Norwood, MA: Artech House, 1997.
- [2] B. A. Munk, *Frequency Selective Surfaces: Theory and Design*. New York, NY, USA: Wiley, 2000.
- [3] P. C. Kim, D. G. Lee, I. S. Seo, and G. H. Kim, "Low-observable radomes composed of composite sandwich constructions and frequency selective surfaces," *Composites Science and Technology*, vol. 68, pp. 2163-2170, 2008.
- [4] H. Chen, X. Hou, and L. Deng, "Design of frequency selective surfaces radome for a planar slotted waveguide antenna," *IEEE Antennas and*

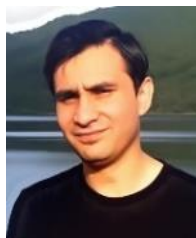


- Wireless Propagation Letters*, vol. 8, pp. 1231-1233, 2009.
- [5] Y.C. Chang, "Low radar cross section radome," US Patent 6,639,567B2.
- [6] E. L. Pelton and B. A. Munk, "A streamlined metallic radome," *IEEE Transactions on Antennas and Propagation*, vol. 22, pp. 799-803, 1974.
- [7] H. Zhou, S. Qu, B. Lin, J. Wang, H. Ma, and Z. Xu, "Filter-antenna consisting of conical FSS radome and monopole antenna," *IEEE Transactions on Antennas and Propagation*, vol. 60, pp. 3040-3045, 2012.
- [8] W. S. Arceneaux, R. D. Akins, and W. B. May, "Absorptive/transmissive radome," US Patent 5,400,043, 1995.
- [9] F. Costa and A. Monorchio, "A frequency selective radome with wideband absorbing properties," *IEEE Transactions on Antennas and Propagation*, vol. 60, no. 6, pp. 2740-2747, June 2012.
- [10] Q. Chen, J. Bai, L. Chen, and Y. Fu, "A miniaturized absorptive frequency selective surface," *IEEE Antennas and Wireless Propagation Letters*, vol. 14, pp. 80-83, 2015.
- [11] S. Abbasi, J. Nourinia, C. Ghobadi, M. Karamirad, and B. Mohammadi, "A sub-wavelength polarization sensitive bandstop FSS with wide angular response for X- and Ku-bands," *International Journal of Electronics and Communications*, 2018.
- [12] W. T. Wang, S. X. Gong, X. Wang, H. W. Yuan, J. Ling, and T. T. Wan, "RCS reduction of array antenna by using bandstop FSS reflector," *Journal of Electromagnetic Waves and Applications*, vol. 23, nos. 11-12, pp. 1505-1514, 2009.
- [13] N. Liu, X. Sheng, C. Zhang, J. Fan, and D. Guo, "Design of FSS radome using binary particle swarm algorithm combined with pixel-overlap technique," *Journal of Electromagnetic Waves and Applications*, vol. 31, no. 5, pp. 522-531, 2017.
- [14] P. Kong, X. W. Yu, M. Y. Zhao, Y. He, L. Miao, and J. J. Jiang, "Switchable frequency selective surfaces absorber/reflector for wideband applications," *Journal of Electromagnetic Waves and Applications*, vol. 29, no. 11, pp. 1473-1485, 2015.
- [15] C. Bakshi, D. Mitra, and S. Ghosh, "A frequency selective surface based reconfigurable rasorber with switchable transmission/reflection band," *IEEE Antennas and Wireless Propagation Letters*, vol. 18, no. 1, pp. 29-33, Jan. 2019.
- [16] Q. Chen, D. Sang, M. Guo, and Y. Fu, "Miniaturized frequency-selective rasorber with a wide transmission band using circular spiral resonator," in *IEEE Transactions on Antennas and Propagation*, vol. 67, no. 2, pp. 1045-1052, Feb. 2019.
- [17] Z. Wang, et al., "A high-transmittance frequency-selective rasorber based on dipole arrays," in *IEEE Access*, vol. 6, pp. 31367-31374, 2018.
- [18] W. Yu, et al., "Dual-polarized band-absorptive frequency selective rasorber using meander-line and lumped resistors," in *IEEE Transactions on Antennas and Propagation*, vol. 67, no. 2, pp. 1318-1322, Feb. 2019.
- [19] Y. Zhang, B. Li, L. Zhu, Y. Tang, Y. Chang, and Y. Bo, "Frequency selective rasorber with low insertion loss and dual-band absorptions using planar slotline structures," in *IEEE Antennas and Wireless Propagation Letters*, vol. 17, no. 4, pp. 633-636, Apr. 2018.
- [20] H. Ahmad, M. U. Khan, F. A. Tahir, and R. A. Bhatti, "A miniaturized frequency selective radome with wide absorption response above X-band," *Progress in Electromagnetics Research Symposium*, Singapore, vol. 2017, pp. 1424-1427, 2017.
- [21] H. Ahmad, M. U. Khan, F. A. Tahir, R. Hussain, and M. S. Sharawi, "Microwave absorber using single-layer FSS with wideband operation above the x-band," *12th European Conference on Antennas and Propagation (EuCAP 2018)*, London, pp. 1-3, 2018.
- [22] W. Wu, Y. Ma, X. Zhang, C. Li, and N. Yuan, "An ultrathin and narrow bandpass frequency selective radome with wide reflection bands," *AEU - International Journal of Electronics and Communications*, vol. 102, pp. 35-40, Apr. 2019.
- [23] P. Xiao, J. Xu, and Y. Han, "Design of dual-polarized frequency selective absorbers," in *2018 International Applied Computational Electromagnetics Society Symposium - China (ACES)*, pp. 1-2, 2018.
- [24] Y. Li, Q. Guo, L. Chen, and Z. Li, "Design of a frequency selective surface with a transmissive window and two bidirectional absorptive bands," in *2018 International Applied Computational Electromagnetics Society Symposium - China (ACES)*, pp. 1-3, 2018.
- [25] Q. Guo, Z. Li, J. Su, L. Y. Yang, and J. Song, "Dual-polarization absorptive/transmissive frequency selective surface based on tripole elements," *IEEE Antennas and Wireless Propagation Letters*, vol. 18, no. 5, pp. 961-965, May 2019.



**Hamza Ahmad** received a bachelor's degree in Electrical (Communication) Engineering from the University of Engineering and Technology, Peshawar, Pakistan, in September 2014, an M.S. degree in Electrical Engineering from NUST Islamabad, Pakistan in 2017. He was also a

Research Fellow at RIMMS NUST, Islamabad, Pakistan from September 2016 to August 2017. Currently he is a Lecturer at Gandhara Institute of Science and Technology Peshawar, Pakistan.



**MuhibUr Rahman** received a bachelor's degree in Electrical (Communication) Engineering from the University of Engineering and Technology, Peshawar, Pakistan, in September 2014, an M.S. degree in Electrical Engineering from NUST Islamabad, Pakistan in March 2016.

He worked as a Research Assistant in Lahore University of Management Sciences, and Dongguk University, Seoul, South Korea. Currently, he is working toward his Ph.D. degree in Polytechnique Montreal, Canada. He published a number of index journals and taken various patents. He is an active reviewer of various well reputed antenna and microwave journals.



**Shahid Bashir** received the B.Sc. degree in Electrical Engineering from the University of Engineering and Technology Peshawar (UET Peshawar), Peshawar, Pakistan, and the Ph.D. degree in Mobile Communications from Loughborough University, Loughborough, U.K., in

2009. He is currently an Assistant Professor with the Electrical Engineering Department, UET Peshawar. He has published in various reputed journals and conferences.



proceedings.

**Wajid Zaman** received an M.S. degree in Electrical Engineering from NUST Islamabad, Pakistan in 2017. His research interest includes multi-band antennas, wide band antennas, and radome. He published various antenna papers in well reputed journals and conference



**Fauziahanim Che Seman** received the degree in Electrical Communication Engineering from Universiti Teknologi Malaysia in 2001, the master's degree from Universiti Tun Hussein Onn Malaysia in 2003, and the Ph.D. degree from the Queen's University of Belfast, U.K., in 2011.

After the Master's degree, she joined the Faculty of Electrical Engineering, Universiti Tun Hussein Onn Malaysia as a Lecturer, where she is currently an Associate Professor with the Research Center of Applied Electromagnetic. She has published number of index journals and conference proceedings and taken various patents.